CONSERVATION SCIENCE IN MEXICO'S NORTHWEST

ECOSYSTEM STATUS AND TRENDS IN THE GULF OF CALIFORNIA

Elisabet V. Wehncke, José Rubén Lara-Lara,
Saúl Álvarez-Borrego, and Exequiel Ezcurra
EDITORS

MANGROVE STRUCTURE AND DISTRIBUTION DYNAMICS IN THE GULF OF CALIFORNIA

Francisco J. Flores-Verdugo,[1] John M. Kovacs,[2] David Serrano,[3] and Jorge Cid-Becerra[4]

The structure and distribution of the mangroves in this region are related primarily to the tectonic origin and by both the local weather and hydrological conditions. On the West Coast of the Gulf of California mangroves are limited to small patches of predominantly dwarf sized trees. In contrast, the East Coast of the Gulf, having a larger coastal alluvial plain and numerous rivers, supports a higher mangrove structure and a larger distribution. New technological advances in Earth observation satellites are now improving our ability to map the mangroves within the Gulf. However, without proper field verification, the accuracy of such mapping endeavors cannot be properly assessed. The mangroves in this region have been particularly impacted by hydrologic modifications and thus new efforts that include the use hydrologic modeling have been considered in order to restore them. New techniques that involve genetic microsatellites are also being employed to identify the presence of different mangrove populations within this region.

1. INTRODUCTION

The mangrove forest structure and distribution in the Gulf of California are mainly related to the tectonic origin, the regional weather conditions and the local geomorphology and hydrological conditions. This region is characterized mainly by a mixture of arid ecosystems with deciduous tropical forest. The States surrounding the Gulf of California are Baja California and Baja California Sur (west coast Gulf of California), Sonora, Sinaloa and Nayarit (east coast Gulf of California).

The mean annual rainfall is less than 600 mm, but the range of annual variations is considerable (200 to 800 mm/year) and is in accordance to the number and

intensities of hurricanes/tropical storms which reach the coast. The hurricane belt is considered to be in the area of the mouth of the Gulf of California because more than 80% of annual tropical depressions-hurricanes of the Oriental Pacific occur in this region.

The tectonic state of the region is considered as neo-trailing-edge coast (Inman and Nordstrom 1971, Carranza-Edwards *et al.* 1975). The west coast of the Gulf of California produces an absence or a very narrow continental shelf (1 to 5 km) with predominantly rocky shores and small coastal lagoons. Combined with the arid climatic conditions, mangrove structure and distribution is limited to small patches of mangroves predominantly dwarf mangrove (< 2m height) with a narrow fringe mangrove less than 4 meters high adjacent to tidal channels and coastal lagoons. In contrast, the east coast of the Gulf of California (Sonora, Sinaloa and north of Nayarit) contain larger coastal alluvial plains and numerous rivers which provide for a higher mangrove structure (5 to 12 m height) and distribution with climatic conditions that vary from arid to sub-humid. Consequently, some of the most extensive mangrove stands and seasonal floodplains of the Pacific coast of the Americas are located in this region (Marismas Nacionales in Sinaloa and Nayarit).

The climate of this region varies from temperate arid (Sonora and both Baja California), warm (mean annual temperature > 26 C) and semi-arid to warm sub-humid for the rest of the region (Sinaloa, Nayarit, 800–1200 mm, Garcia 1973). Typically heavy seasonal rainfalls occur mainly in the summer months (July to September) and these are strongly influenced by hurricanes. Evaporation rates ranges from 1800–2000 mm. Most of the rivers of this region have a small hydrological basin with the exception of the Yaqui and Mayo rivers basins in Sonora and the Santiago river in Nayarit, flowing seasonally to intermittent from south to north (Arriaga-Cabrera *et al.* 1998b, Atlas 1990).

The intertidal vegetation consists predominantly of 4 species of mangroves: red mangrove (*Rhizophora mangle*), white mangrove (*Laguncularia racemosa*), black mangrove (*Avicennia germinans*) and button mangrove (*Conocarpus erectus*). In Baja California Sur, local peoples consider another tree (*Maytenus phyllanthoides*) as "sweet mangrove". Mangroves are discontinuously distributed along the region with few extensive mangrove forests in Topolobampo-Ohuira, San Ignacio-Navachiste-Macapule, Bahía de Santa María and Ensenada del Pabellón in Sinaloa and in Marismas Nacionales along the border of Sinaloa and Nayarit (see Figure 1: 2-5 and 7, Flores-Verdugo 1992). In the Baja California east coast, the mangroves are mainly fringe mangrove of a few meters width. An important factor that defines the species and structural development of mangroves in this region is the soil salinity. Black mangrove (*A. germinans*) is the most tolerant to high soil salinities (> 50 < 70 psu)

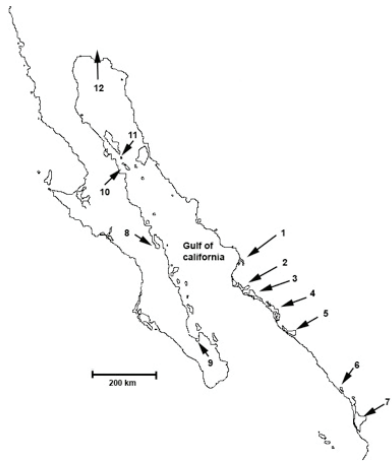

FIGURE 1. The Gulf of California and the location of the sites of reference: 1. Jitzamuri-Bacorehuis (Sinaloa), 2. Topolobampo-Ohuira bay (Sin.), 3. San Ignacio-Navachiste-Macapule bays (Sin.), 4. Santa María Bay (Sin.), 5. Ensenada del Pabellón coastal lagoon (Sin.), 6. Huizache-Caimanero coastal lagoon (Sin.), 7. Marismas Nacionales estuarine complex (Sin.-Nayarit), 8. Bahía de Concepción (BCS), 9. Ensenada de La Paz (BCS), 10. Bahía de los Ángeles (BC), 11. Coronado (Smith) island (BC) and 12. Colorado delta (BC, Sonora).

and thus the most dominant dwarf mangrove species (< 2 m height) landwards of a mixed very narrow fringe forest of red, white and black mangrove (> 4 m). This later fringe mangrove is found along the edge of the lagoons and tidal channels where soil salinities are < 50 psu. In general, fringe and dwarf mangroves are associated with extensive hyperhaline seasonal flood plains ("marismas") with or without saltwort *Salicornia* spp. and *Batis maritima* or even with salt pans (> 90 psu, Jiménez, 1998).

The forest structure increases towards the south as the rainfall increases and in areas with important freshwater input from rivers (Flores-Verdugo *et al.* 1992).

Mixed freshwater wetlands of cattail (*Typha* spp.) with mangroves can be found in Chiricahueto–Ensenada del Pabellón and Patolandia in Bahía de Santa Maria, Sinaloa.

The region has several coastal lagoons and, according to Lankford´s (1977) classification, are predominantly of the type Barred Inner Shelf subtype Gilbert-Beaumont Barrier lagoons and in Nayarit the subtype Strand Plain Depression with multiple sand barriers in Marismas Nacionales (Teacapán-Agua Brava-Las Haciendas). In the latter, Curray *et al.* (1969) estimated the presence of more than 128 sub parallel ridges formed by successive accretion by sand deposition when the transgression of the eustatic sea level slowly rose several times between 3,600 and 4,750 B.P.

The presences of numerous shell middens ("conchales") of *Tivela* sp. and oyster (*Crassostrea* spp.) of more than 1,500 year BP in the region of Marismas Nacionales indicates human presences since those times.

The sand beaches are a continuous component in Sonora, Sinaloa, and Nayarit interrupted only by the rivers / lagoons inlets. Baja California coast is predominantly a rocky coast with small and narrow beaches backed with small coastal lagoons surrounded by mangroves from Bahía de los Ángeles and Coronado (Smith) island including Concepción Bay, to Ensenada de La Paz and Los Cabos) (see Figure 1: 8-11).

There are several coastal classifications for this part of Mexico related to geological, tectonic, morphogenesis and biological characteristics (Carranza-Edwards *et al.* 1975, Lankford (1977), Flores-Verdugo *et al.* (1992) and Contreras-Espinosa (1993). Ortiz-Perez and Espinosa-Rodriguez (1990) also consider a geodynamical classification. According to those authors the region can be classified as being predominantly Prograding Coast (advancing of the coastline toward the ocean by sedimentation). However, the opposite occurs in one point, specifically in front of the Colorado river-estuary where it is related to deltaic inactivity or submersion (see Figure1: 12). One important characteristic of several shallow coastal lagoons of this region is the exposure of extensive areas to the air as a consequence of the high evaporation rate during the dry season. For example, more than 70% of the surface of Huizache-Caimanero is dried during the dry season and, moreover, the cracking of the exposed soil is believed (Arenas & de la Lanza, 1981) to have an important role in the release of nutrients when it is subsequently flooded (see Figure 1: 6).

The Teacapán-Agua Brava-Marismas Nacionales is the most extensive mangrove area of this region (150,000 ha). It is also quite unique with several large homogeneous areas of white mangrove (*L. racemosa*). The region has been studied in aspects of mangrove structure, litterfall, leaf degradation, aquatic primary productivity and fish community dynamics presenting densities as high as 3, 203 trees ha^{-1}, basal areas from 14 to 29.6 m^2 ha^{-1} and litterfall near to 1 kg m^2 yr^{-1}. One interesting aspect of this system is the high concentrations of humic substances that develop during the wet season (> 150 mg l^{-1}) from the mangroves detritus resulting in a red color of the water (Flores-Verdugo *et al.* 1992). The environmental implications of the high concentrations of humic substances in this region are still unknown. The litterfall of several fringe mangroves of the region is also considerable high compared to other regions (*i.e.* Caribbean). There is no clear explanation why mangroves with such relatively low forest structure are as productive in litterfall as well developed riverine mangroves (Flores-Verdugo *et al.* 1987, 1993, Felix-Pico *et al.* 2006).

Earth observational satellites for mangrove monitoring and mapping: Potential use and challenges for Northwest Mexico. In order to properly manage and monitor mangrove forests it is essential that updated maps, indicating the extent and condition of these forested wetlands, be available to resource managers. Such maps might be extremely important for identifying ideal locations for mangrove restoration or for simply examining impacts on mangroves resulting from hydrological modifications, whether natural or anthropogenic. In the past such monitoring activities were extremely costly and time consuming often involving traditional techniques of aerial photographic interpretation and/or extensive in the field biophysical data collection (*e.g.* tree height, tree diameter). This later approach is particularly logistically difficult given the remoteness of mangrove forests and the harsh environment conditions associated with these forests (*e.g.* tidal fluctuations, loose substrate). Consequently, it is no surprise that there have been numerous attempts, even in Northwest Mexico (Kovacs *et al.* 2001, Berlanga-Robles and Ruiz-Luna 2002, Kovacs *et al.* 2004, Fuente and Carrera 2005, Kovacs *et al.* 2005, Kovacs *et al.* 2006, Kovacs *et al.* 2008a, Kovacs *et al.* 2008b, Kovacs *et al.* 2009), to use Earth observational satellites to replace this aspect of mangrove forest management.

Earth observational satellites can provide repetitive coverage of the most remote mangrove forests and they can be readily processed as digital data (*i.e.* manipulated) to provide digital classified maps of mangrove types (*e.g.* dwarf mangrove, tall mangrove). In particular the focus so far has been the use of traditional optical remote sensing platforms such as LandSat MSS, LandSat TM, SPOT and more recently the higher spatial resolution satellites (*e.g.* 1 m on the ground pixel size) such as IKONOS, QuickBird and GeoEye (Walters *et al.* 2008). These optical sensors use the reflection of the Sun's energy off the Earth surface to collect and analyze information on land cover/use features including mangroves. These sensors collect information from the visible area of the electromagnetic spectrum (~400–700 *nm*) as well as the non-visible near infrared (~760–900 *nm*). This later region is extremely useful for monitoring the health of vegetation including mangroves. In particular, very high reflectance in the infrared is indicative of relatively healthy plants and, conversely, low reflectance in the infrared occurs for unhealthy or senescent plants. In contrast, water almost completely absorbs this type of electromagnetic energy. For comparative sake, Figure 2 shows an image of Isla La Palma (Sinaloa) taken using the QuickBird Earth observation satellite in both natural color composite and false color infrared composite. The very bright red in the later image is indicative of very healthy mangrove along the edge of the island which contrasts with the very poor condition of mangroves located more inland that has a very low red coloration.

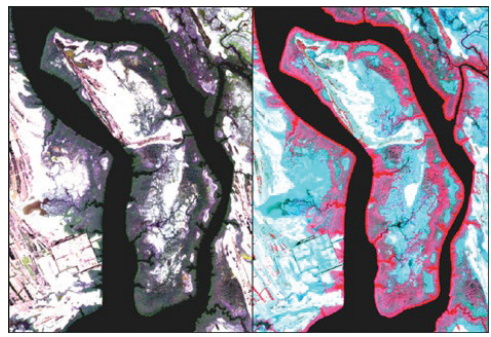

FIGURE 2. Linear enhanced QuickBird Earth observing satellite images of Isla la Palma (22°37'N, 105°40' W) using a natural color composite (left) and a false color infrared composite (right).

Consequently, these data can be used to map the state of mangrove forests (*e.g.* healthy, poor condition, dead) or to extract information associated with mangrove biomass such as Leaf Area Index (LAI) which is a good proxy for health. Alternatively, these data can also be used to determine hydrological data associated with mangroves, including areas of open water which appear black in the images due to its high absorption of infrared energy.

The selection of Earth observing satellite for mangrove monitoring does alter the quality of data that can be derived. With regards to the optical sensors, the very high spatial resolution images (*e.g.* IKONOS, QuickBird), which are often shown in Google Earth, are required in order to map mangroves at the species level (*e.g.* separate *L. racemosa* from *R. mangle*) or for extracting LAI. For example, IKONOS and QuickBird data have been used successfully to map estimated mangrove LAI for the Agua Brava (Kovacs *et al.* 2005) and the Teacapan Estuarine (Kovacs *et al.* 2009) areas, respectively, within the Marismas Nacionales. However, these satellite data are expensive, have limited swath coverage, and historical records are limited. In contrast, the traditional sensors such as LandSat and SPOT have larger swath coverage, are considerably cheaper if not free, and have been recording images of the Earth for decades. The key limitation for these coarser spatial resolution satellites (*e.g.* 30 meter pixel size) is the inability to separate mangroves at the species level. However, these traditional data can be used to separate and map mangroves from other land features as well as providing qualitative maps of mangrove forest condition (*e.g.* healthy, poor condition, dead). In addition to optical sensors, Synthetic Aperture Radar (SAR) Earth observing satellites are now being assessed as an alternative to optical satellites for mangrove monitoring and mapping. Unlike the optical, these sensors do not rely on the Sun's energy but rather emit and receive

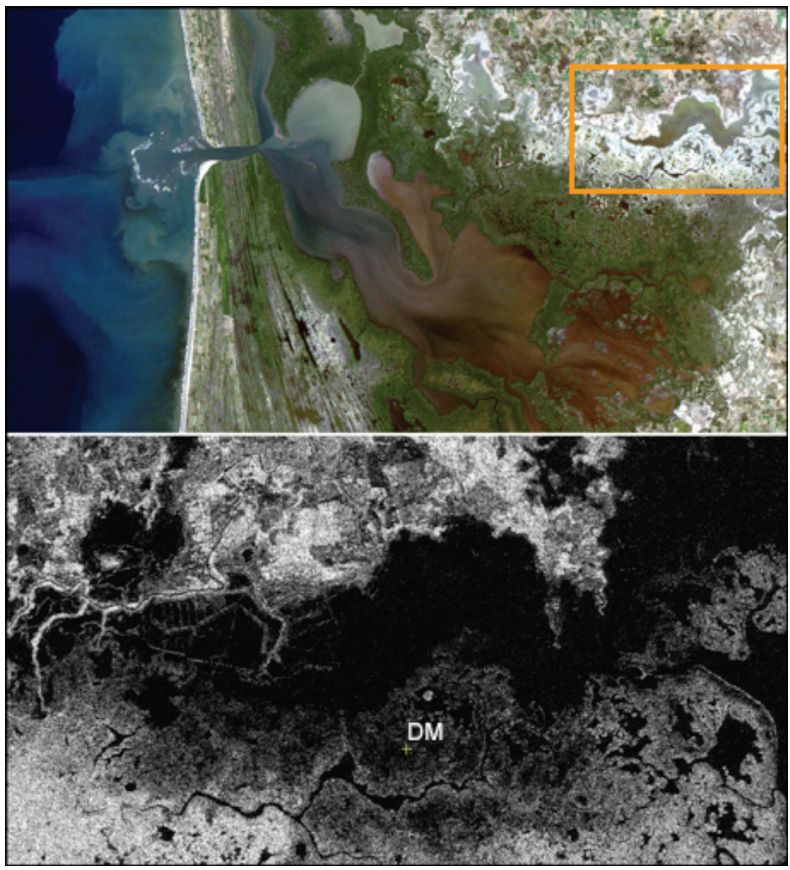

FIGURE 3. An enhanced natural color composite image of the Agua Brava lagoon (22°09' N, 105° 30' W) from the optical sensor (AVNIR) of the ALOS Earth Observing satellite (top). Below is an enhanced SAR (*i.e.* radar) image, the subset shown above, using the radar sensor (PALSAR) of the same Earth observing satellite. Note that the dead mangrove (DM) region is readily identified by both sensors.

their own microwave energy (*e.g.* RadarSat-2 C-band 5.4 *GHz*). As a result they can register mangroves at night and, unlike optical sensors, can register through clouds. In addition, SAR can provide information on the geometry and dielectric properties of the target it is measuring. Although promising, only a few studies, many of them conducted in Northwest Mexico (Kovacs *et al.* 2006, Kovacs *et al.* 2008a, Kovacs *et al.* 2008b), have so far examined SAR in relation to mangrove forest monitoring. The results suggest that SAR is particularly useful, either alone or in conjunction with optical satellite data, for monitoring the health of mangrove forests undergoing

degradation. For example, in Figure 3 the large dead white mangrove (*L. racemosa*) area is just as easily identified in the SAR image as in the optical image. Specifically, the healthy trees are white (*i.e.* radar intensity) in the SAR image because the leaves deflect the emitted radar signal back to the satellite. In contrast, in the absence of leaves there is no signal from the dead stands as the emitted radar signal (L-band, HV polarimetry) simply deflects away off the ground with no return to the satellite.

Although many studies have shown the great potential for mapping and monitoring mangroves with Earth observing satellites, one should always be vigilant of the mapping results. This is especially true if no field verification (*i.e.* accuracy assessment) was conducted in conjunction with the satellite image mapping procedure. An example of conflicting results from satellite mapping of mangroves can be found for the Sinaloan section of the Marismas Nacionales, which is considered the largest mangrove system of Northwest Mexico, if not of the Pacific Coast of the Americas. Four recent mangrove mapping exercises all using traditional LandSat Earth observing satellite data have resulted in conflicting results. Two studies (Berlanga-Robles and Ruiz-Luna 2002, Fuente and Carrera 2005), which employed a simple mangrove/non-mangrove classification approach have indicated a considerable extent of mangrove forest and, moreover, that over time these forests have been expanding in this system. In stark contrast, studies by Kovacs *et al.* (2001, 2008b), using a more elaborate mangrove classification system (*e.g.* dead mangrove, poor condition mangrove), indicated an extremely degraded mangrove system that appears to be worsening. Using a subset of this study area, Isla La Palma, we see in Figure 4 the contrasting results from these conflicting approaches. Although considered mangroves by Fuente and Carrera (2005), many of these mangrove stands are in fact dead or in a considerable state of degradation. Using higher spatial resolution satellite data this poor state of mangrove health for the Isla La Palma has recently been confirmed (Kovacs *et al.* 2009). Moreover, recent SAR images are also suggesting a poor state for this important mangrove system. In Figure 5, it is apparent that large areas in the northern region of Marismas Nacionales (lagoon Agua Grande) considered as mainly mangrove forest by some researchers (Berlanga-Robles and Ruiz-Luna 2002, Fuente and Carrera 2005) are in fact degraded mangrove or saltpan since they show little or no radar backscatter signal (*i.e.* black tone) in the SAR image.

In summary, the use of Earth observing satellites to map and monitor mangroves is now becoming the norm in Mexico as in other countries. The current transition in the use of traditional coarser spatial resolution optical satellites to higher spatial resolution ones will improve our ability to map and monitor these forests. Moreover, with the advent of newer SAR systems being used in conjunction with optical sensors it is anticipated that the accuracies of mapping mangrove forests will improve

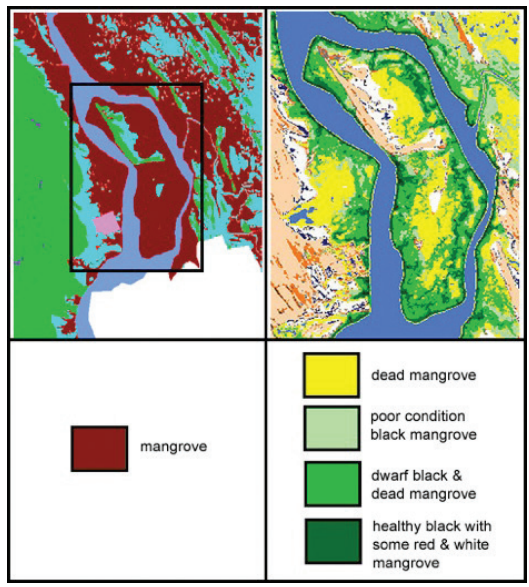

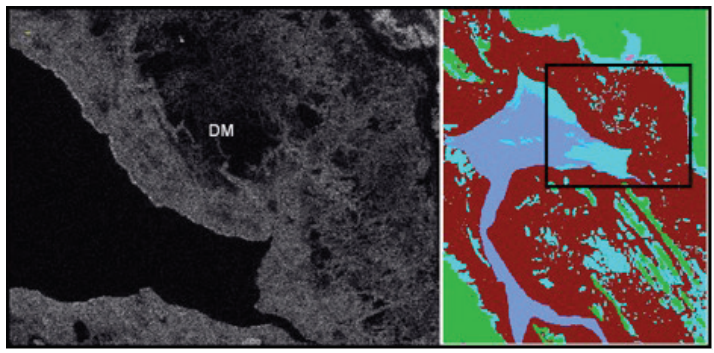

FIGURE 4 (ABOVE). A comparison of mangrove classifications for the Isla la Palma based on LandSat Earth observing satellite data as employed by Fuente and Carrera (2005) on the left (modified from DUMAC 2005) and, on the right, by Kovacs *et al.* (2008b). FIGURE 5 (BELOW). A comparison of a recently classified map based on LandSat data (Fuente and Carrera 2005) indicating mangroves in the dark red color (image on right) with an enhanced ALOS PALSAR image (image on left). Note the large area of dead mangrove (DM) and saltpan in the PALSAR image which is identified mainly as mangrove in the classified map.

considerably. Finally, it is important to reiterate that although Earth observing satellites can be extremely beneficial for mapping the extent and condition of mangroves of Northwest Mexico, without proper field verification (*i.e.* map accuracy assessment) the results from such procedures should be taken with some level skepticism.

2. MANGROVE DISTRIBUTION, HYDROPERIOD, HUMAN IMPACTS AND MITIGATION

With few exceptions the restoration of mangroves in the northwest of Mexico considered only reforestation without any knowlwdge of the local hydrological dynamics and thus have been very prone to failure (Toledo *et al.* 2001, Benitez-Pardo 2004, and Strangman *et al.* 2008). It is postulated that mangrove distribution is affected by microtopography, frequency of tidal flooding and salinity (Cintrón *et al.* 1985, Jimenez and Lugo 2000). In particular, the type of coastal wetland found is often determined by the hydroperiod and the level of salinity present. The effects of tides are considered important factors in mangrove development and growth, with the tides helping to recycle nutrients and lowering hypersaline conditions (Twilley and Day 1999). The hydroperiod affects the productivity and distribution of mangroves, which according to Flores *et al.* (2006) is determined by both the tides and the microtopography. Owing to their nature, mangroves develop best on coastal plains with low topographic gradients. Such areas allow freshwater or seawater to penetrate but also help to determine a flooding gradient which produces a selective response for each mangrove species (Monroy-Torres 2005). This in turn allows for selective mangrove colonization (mangrove zonation). Examples of activities that can hinder mangrove growth include interrupting mangrove irrigation periods, modifying adjacent water salinity, influencing the flooding surface in the rising rivers and altering tide fluctuation by carrying out engineering infrastructure (*e.g.* roads, levees). The effects of such activities can include the reduction in growth and/or development of mangrove zones as well as the potential development of dead mangrove zones. Mangroves of the Northwest have been particularly affected by such hydrologic modifications. New modeling techniques may be used to assist in restoration activities following such occurrences or how they can be used to predict potential impacts to mangroves prior to such constructions by simulating the hydroperiods.

3. TOPOLOBAMPO BAY (THE MARIVI BEACH)

In the 1960's, access to Marivi beach by the inhabitants of Los Mochis and Topolobampo was impeded by the presence of a dense forest of dwarf mangrove and seasonal floodplains. In order to allow easy access, the authorities constructed a road connecting the port of Topolobampo to Marivi Beach. The construction of a 319 m road track sectioned off the El Zacate estuary (see Figure 6). Those responsible for the work left a channel less than 8 meters wide which in fact now connects El Zacate estuary to the main water body. However, this engineering work proved inadequate

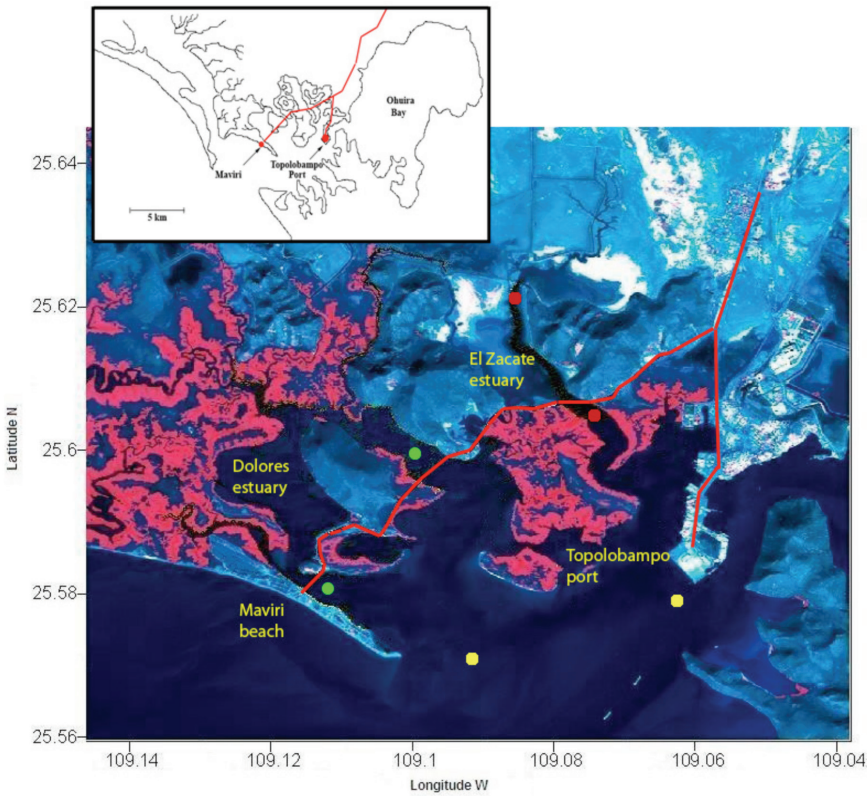

FIGURE 6. Study area. Details of the Topolobampo lagoon, El Zacate and Dolores estuaries. Yellow points represents the sea level measurement sites in the open borders. Red points refer to the internal and external reference points associated to the Zacate estuary. Red line refer the highway and red colour to mangrove areas. The green points refer to the internal and external reference points for the Dolores estuary. The term estuary is translated from the Spanish word "estero" which corresponds predominantly to tidal channels and seasonal floodplains or "marismas" (for location see Figures 1-2).

as it reduced the hydraulic conductivity considerably, resulting in the destruction of about 350 hectares of mangroves.

4. NUMERICAL MODEL

A mathematical model was used to simulate the hydrological conditions of the study zones before and after the hydrological changes caused by human activities. The mathematical model used in these studies was previously applied in other regions such as the Gulf of California (Carbajal and Backhaus 1998) and Santa María del

Oro Lake (Serrano *et al.* 2002). The model is non-linear, with both the equations of momentum and continuity vertically integrated. These equations are solved semi-implicitly, using finite differences in an Arakawa C-grid. The bottom friction is parameterized in an implicit form, and the friction coefficient changes with depth (Baumert and Radach 1992). A complete description of the model can be seen in Carbajal (1993).

The computational grid used to schematize the lagoon systems has a resolution of $\Delta x = \Delta y = 10$ m. The eddy viscosity coefficient was calculated in agreement with Schwiderski (1980). The lagoon systems were forced by the sum of the seven main tide components in the open boundaries. The amplitude and the phase of the seven harmonics were linearly interpolated of the port of Topolobampo the amplitude and phase recorder for this port was used (UNAM 1994).

$$(1)\quad \frac{\partial U}{\partial t} + \frac{U}{(H+\zeta)}\frac{\partial U}{\partial x} + \frac{V}{(H+\zeta)}\frac{\partial U}{\partial y} - fV = -g(H+\zeta)\frac{\partial \xi}{\partial x} + A_H \nabla_h^2 U - \tau_b^x,$$

$$(2)\quad \frac{\partial V}{\partial t} + \frac{U}{(H+\zeta)}\frac{\partial V}{\partial x} + \frac{V}{(H+\zeta)}\frac{\partial V}{\partial y} + fU = -g(H+\zeta)\frac{\partial \xi}{\partial y} + A_H \nabla_h^2 V - \tau_b^y,$$

$$(3)\quad \frac{\partial \xi}{\partial t} + \frac{\partial U}{\partial x} + \frac{\partial V}{\partial y} = 0.$$

Variables to resolve the elevation of the sea free surface flows ζ and their transport U (in the zonal x direction) and V (in the meridian direction y). H is the depth (bathymetry), t is time, g acceleration due to gravity, A_H horizontal coefficient of turbulent viscosity, ∇_h^2 horizontal laplaciano operator, τ_b bottom friction and f Coriolis parameter.

5. BATHYMETRY

The bathymetric matrix was carried out by capturing about 3,000 sampling points, registering their depth and their geographical position. Measurements in the Maviri zone were carried out by staff from the Topolobampo Oceanographic Research Station of the Mexican Navy. This information was then submitted to MATLAB graphics. A matrix of 658 lines with 731 columns was constructed, with a spatial resolution of $\Delta x = \Delta y = 10$ m, where each node number represented the depth of the study zone (see Figure 7).

6. TIDAL SIMULATION

The open borders (red line, Figure 7) were calibrated to the tides registration of Topolobampo port, Sinaloa, which can be described as a good approximation with the sum of: M_2, S_2, K_1, O_1, N_2, K_2 y P_1. The sea level time-series reproduced in the

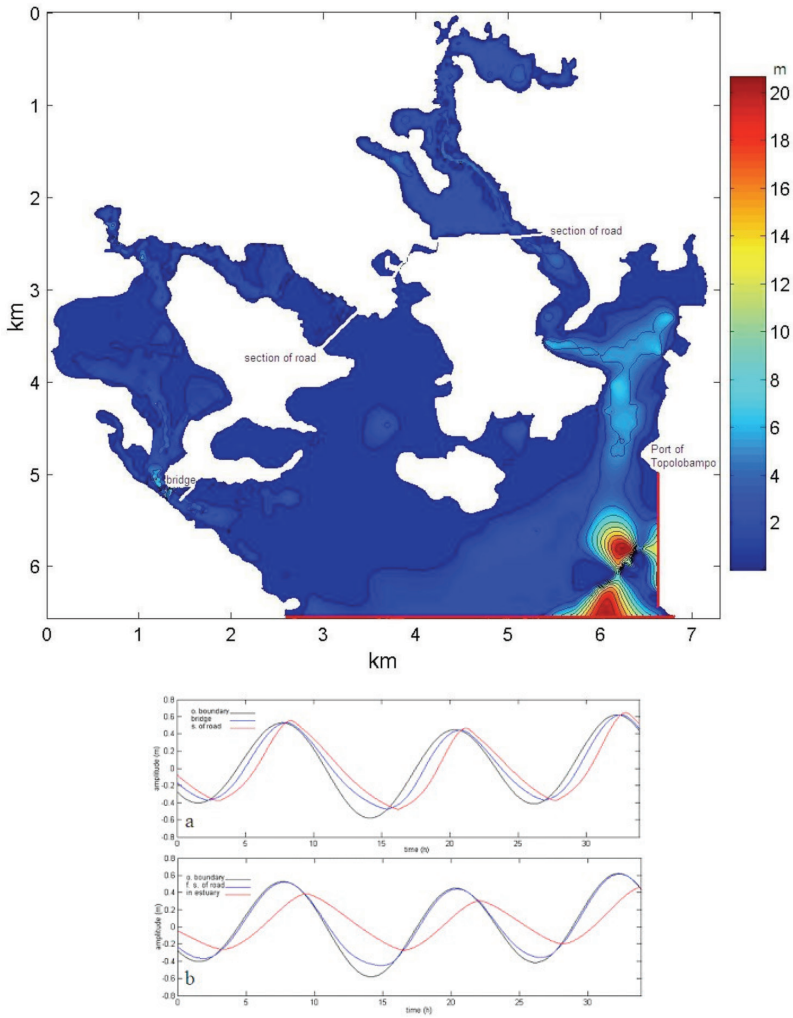

FIGURE 7 (ABOVE). Bathymetry of the study area: Topolobampo-Maviri. Red lines indicate the open borders used for the numerical model. Two meter depth intervals were used. FIGURE 8 (BELOW). A time series of tidal activity under actual conditions (*i.e.* with the highway lanes): (a) Dolores and (b) El Zacate estuaries. Black line is the open border (main water body), blue line outside the estuaries and red line inside the estuaries (see Figure 6).

open borders of the numerical model is shown in Figures 8 and 10 (black lines). This time-series comprises a ~35 hr simulation, within a spring tide time interval reported for Topolobampo Port. The maximum height was 622 mm and the minimum - 580 mm, both referred to as Mean Sea Level (MSL).

7. ACTUAL CONDITIONS

Real time-series analyses of sea-level conditions (*i.e.* includes highway lanes and bridge) for Dolores estuary are shown in Figure 8a. The black line represents sea level in a point situated in open sea (yellow points, Figure 6); the blue lines show sea level in a point situated in front of the bridge, in the inlet of Dolores estuary (external green point, Figure 6) and the red line refers to the sea level in the point situated in the interior of the estuary, close to the highway lane (internal green point, Figure 6). Three time-series of sea level with actual conditions (*i.e.* includes highway lanes and bridge) for Zacate estuary are shown in Figure 8b. The black line represents the sea level in a point situated in the open sea (yellow point, Figure 6); the blue line shows sea level in a point situated in front of the highway lane which divides the Zacate Estuary (red external point, Figure 6) and the red line, refers to the sea level in a point situated in the interior of the same estuary (internal red point, Figure 6). No significant differences were obtained in the time-series analysis for sea-level in the interior and exterior of Dolores estuary. The registered time-series in the interior of the estuary showed a tidal lag of approximately 20 minutes as well as an increase in height of 23 mm in respect of the series captured opposite the bridge. This result suggests that the tidal flooding zone surrounding the estuary did not appear to be affected, thus sustaining a healthy mangrove ecosystem. Therefore, constructing bridges or placing channels in the highway lane that divides the Dolores estuary are unnecessary.

On the other hand, sea-level time-series in the internal and external points of the Zacate estuary indicate significant differences. The registered time series in the internal points of the estuary shows a tidal lag of approximately 95 minutes as well as a 200 mm reduction in tidal range according to the time registered opposite the highway lane (external point). This result suggests that the tidal flooding zone surrounding Zacate estuary is affected, thus modifying the hydrological conditions of the mangrove. Figure 9 depicts a three-dimensional image of the sea-level elevation in the study zone. The time fluctuations and decrease of the sea-level are considerable in Zacate estuary as compared to the main water body (see Figure 9b).

8. NATURAL CONDITIONS (BEFORE THE HIGHWAY)

So as to understand the hydrological conditions before the highway in the study zone, particularly in the estuaries, the bathymetry matrix was also modified. Specifically, values greater than zero were assigned to the dry points that divide the estuaries (highway lanes). The allocated depth was determined by lineal interpolation on the

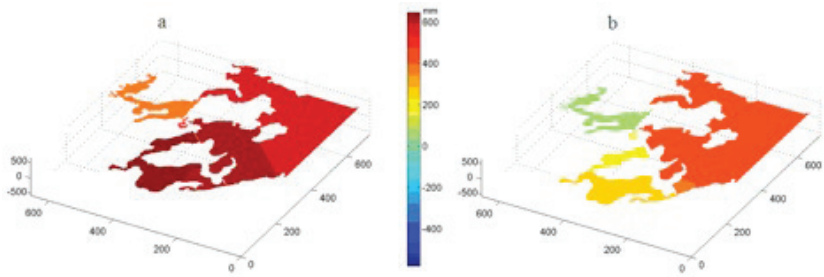

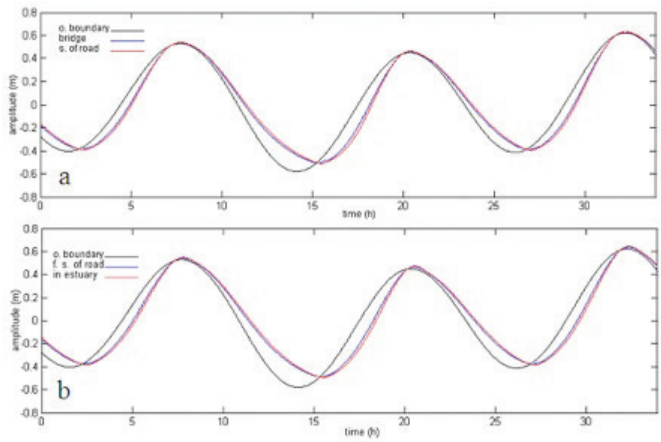

FIGURE 9 (ABOVE). Three-dimensional images of the sea-level fluctuations at Topolobampo-Maviri costal lagoon-mangrove system. El Zacate and Dolores estuaries at high tides (a) and at flow tide (b) for the actual conditions (*i.e.* with highway lanes and bridge). FIGURE 10 (BELOW). A time series of tidal activity under natural conditions (*i.e.* without the highway lanes): (a) Dolores and (b) El Zacate estuaries. Black line is the open border (main water body), blue line outside the estuaries and red line inside the estuaries (Figure 6).

basis of the depth of both sides of the highway lanes. Three time-series at sea-level with "natural" condition (excluding highway lanes) are shown in Figure 10. Likewise, in Figure 8, the black line represents sea-level in a point situated in the open borders; the blue line shows sea-level in a point situated opposite the bridge, in the inlet of Dolores estuary, and the red line refers to sea-level in a point situated in the interior of the estuary, close to where the highway lane was constructed (see Figure 10a). The three points are shown in Figure 6 (green and yellow circles).

The time-series at sea-level with "natural" condition (*i.e.* excluding highway lanes) for Zacate estuary are shown in Figure 10b. The black line represents sea-level in a

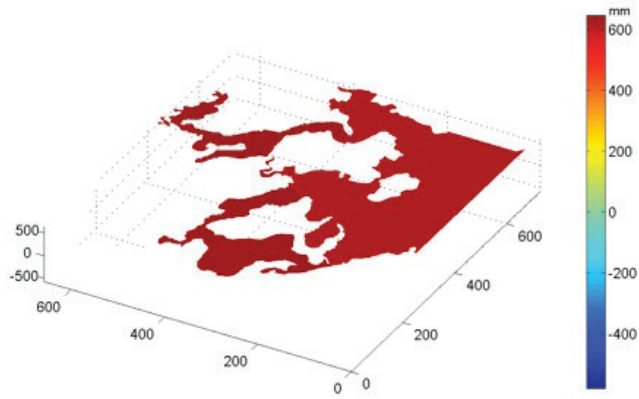

FIGURE 11. Three-dimensional image of the sea-level fluctuations at Topolobampo-Maviri costal lagoon-mangrove system. El Zacate and Dolores estuaries at high tides (a) and at flow tide (b) under "natural" conditions (*i.e.* without highway lanes and bridge). No abnormalities can be seen.

point situated in the eastern open border; the blue line shows sea-level at a point close to where the highway lane was constructed, which divides the Zacate estuary and the red line refers to sea-level in a point situated in the interior of the same estuary. The three points are situated in Figure 6 (red and yellow circles). No significant differences were found in the time-series analysis at sea-level in the interior and exterior of the Dolores and Zacate estuaries. Time-series of the interior of Dolores estuary showed a 2 mm increase in height, however, according to the time-series of the exterior, no important tidal delay was found. On the other hand, the time-series in the interior of Zacate estuary shows an increment of 8 mm in height and a slight tidal lag of less than 1 minute behind the external series. A three-dimensional image of sea-level elevation with natural conditions in the study zone is shown in Figure 11. No significant differences were found for both parameters.

9. RECOMMENDATIONS

The object of implementing a numerical model under natural conditions was to determine the sea-levels in the study zone before the highway lanes were constructed and then to propose the development of new bridges and channels (including dimensions), in a way that the engineering work secures the hydraulic supply (by tides) of the damaged zones. The criteria used for recommending the dimensions of a new bridge in Zacate estuary was to preserve the elevation of the sea level by

TABLE I. Flows, water speed and other parameters for El Zacate on natural conditions, "actual conditions and with the bridge proposal.

	Natural conditions	Actual conditions	Bridge proposal
Depth average	1.73 m	3.3 m	2.7 m
Length	330 m	10 m	70 m
Area	570.9 m^2	33.0 m^2	189.7 m^2
Speed average	0.1687 m s^{-1}	1.6343 m s^{-1}	0.5041 m s^{-1}
Flow	96.31 m^3 s^{-1}	53.93 m^3 s^{-1}	95.63 m3 s^{-1}

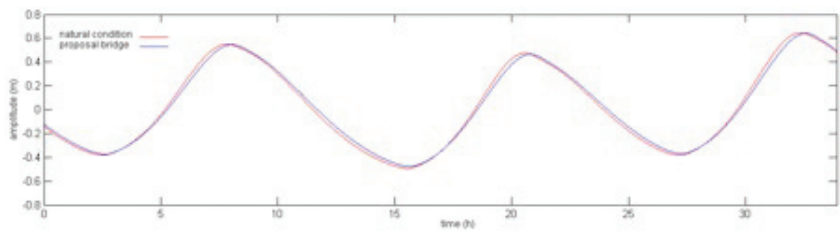

FIGURE 12. A time series of tidal activity under natural conditions (red line) and with the proposed bridge (blue line) in the Zacate estuary.

tides (flooding surface) in accordance to the natural condition. Different numerical experiments were carried out, modifying in each transversal section the proposed bridge (*i.e.* length and depth according to MSL). The numeric model determined that the best solution for Zacate estuary is to construct a bridge measuring 70 m length by 2.7 m depth according to the recommendations of MSL. A time-series at sea-level in the interior of Zacate estuary, with "natural" conditions and with the "construction" of the above described bridge, are shown in Figure 12. Here, the similarity of both series is appreciated. The time-series in the interior of the estuary with the "construction of the bridge" shows a slight decrease in deterioration of less than 5 mm and a slight tidal delay of 14 minutes. On the other hand, the hydraulic conductivity in the entrance of Zacate estuary was calculated under "natural" conditions, actual conditions and the proposed 70 m bridge construction. It should be pointed out that the transversal area was calculated with the actual bathymetry. The results of all three cases are shown in table 1. The results reveal that the proposed bridge project fulfills the conditions similar to natural hydrology before the highway retaining the sea-level at Zacate estuary, with less than 5 mm. The difference in the hydraulic dynamics between natural conditions and the proposed bridge is less than 1%.

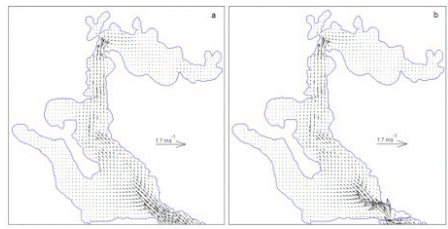

FIGURE 13. Currents distribution and velocities during the flow tide according to the numerical model for El Zacate under natural conditions (a) and with the proposed bridge (b).

The field velocities distribution in the flow tide within Zacate estuary under natural conditions and with the proposed work is shown in Figures 13a and 13b respectively. Both fields have well-known similarities, except in the threshold/entrance/limit of the estuary, which under natural conditions presents a maximum velocity of 57.3 cm s^{-1}, likewise the maximum velocity for the proposed work is 111.2 cm s^{-1}. Then again, we propose that the construction work be carried out between (extreme left of the bridge) at 25 36 23.69" N and 109 04 41.97" W and (extreme right of bridge) 25 36 23.79" N and 109 04 39.46" W, in accordance with the bathymetry and "free" flow. This implicates that the centre of the bridge will be situated at 25 36 23.70 N and 109 04 40.72 W, approximately 20 meters west of the channel.

10. MANGROVE GENETIC CHARACTERIZATION AS A TOOL FOR MANGROVE REFORESTATION

To improve restoration success it is suggested that another technique, related to mangrove genetic characterization be considered. The goal of this mangrove diagnostic is to identify the natural characteristics of the mangrove ecosystem in order to re-establish the damaged areas with the most appropriate mangrove propagules. Before the intensive production of mangrove nursery-reared plants for restoration efforts in Sinaloa, it was deemed important to determine the genetic structure of the four mangrove species naturally distributed in the Northwest of Mexico. The question to resolve was, for the mangrove species, which dispersion via the embryos is influenced by the internal currents of the coastal aquatic systems. Moreover, to present ecological barriers along the latitudinal gradient defined by the geographical position of the aquatic coastal systems of Sinaloa. Without this diagnostic, the empirical restoration efforts could be ecologically dangerous. Specifically, there is the potential, with reforestation efforts, of the presence of the Whalund effect derived from the inbreeding of individuals with a different variance for a number of loci

from different populations of a mangrove species. Based on this concern, a genetic structural diagnostic for Sinaloa coast was carried out in 2006 with the collection of samples taken from the 14 principal aquatic coastal lagoons. Microsatellites makers were used of Rosero-Galindo *et al.* (2002) and Nettel *et al.* (2005) which were standardized for Sandoval-Castro (2008) to *Rhizophora mangle* and *Avicennia germinans*. New ones were designed for *Laguncularia racemosa* and *Conocarpus erectus* (Nettel *et al.* 2007, 2008). The seven microsatellites markers used for red mangrove *R. mangle* were: Rm7 $[(TA)_{14}\ (TGTA)_{2}\ (CA)_{11}\ (TA)_{3}\ (GA)_{4}\ (GA)_{2}]$; Rm11 $[(CT)_{16}\ (CA)_{3}]$; Rm19 $[(AG)_{26}]$; Rm21 $[(CT)_{12}]$; Rm38 $[(CA)_{8}]$; Rm41 $[(GA)_{25}]$ and; Rm46 $[(AT)_{4}\ (GCGT)_{8}\ (GT)_{8}\ (GGAA)_{2}]$. For black mangrove *A. germinans* we used seven microsatellites markers: AgT4 $[(CATA)_{5}\ CATG(CATA)_{9}]$; AgT7 $[(CAT)_{2}\ (AT)_{3}\ (GTAT)_{5}]$; AgT8 $[(TGTA)_{6}]$; AgT9 $[(CA)_{8}\ (GA)_{2}\ (CAGA)_{5}]$; AgD6 $[(ATT)_{4}\ N_{7}(GT)_{15}]$; AgD13 $[(CA)_{10}]$ and; CA_002 $[(CA)_{12}]$. The nine new microsatellites markers for white mangrove *L. racemosa* were: Lr101 $[(CAAT)_{4}\ N_{36}\ (CT)_{5}]$; Lr17 $[A_{9}\ TAAA\ (GAAA)_{7}]$; Lr22 $[(GAGT)_{4}\ (GA)_{6}]$; Lr33br $[(GAAA)_{6}]$; Lr38 $[A_{4}\ G\ A_{6}\ (GAAA)_{7}]$; Lr39br $[(CTTT)_{5}\ N_{6}\ T_{6}\ C\ T_{9}]$; Lr41 $[(CTTT)_{4}]$; Lr42 $[(CTTT)_{5}]$ and; Lr8 $[(GA)_{16}]$. Also we develop ten new microsatellites markers for buttonwood mangrove *C. erectus* : Ce21 $[(GT)_{16}]$; Ce25 $[(CT)_{11}\ N_{24}\ (CT)_{3}\ N_{6}\ (CT)_{11}]$; Ce29fa $[(CT)_{7}]$; Ce32 $[(CTT)_{5}]$; Ce34 $[(CTT)_{8}]$; Ce35 $[(CTT)_{6}]$; Ce42 $[(A)_{9}\ (GAAA)_{4}]$; Ce44 $[(CT)_{11}]$; Ce46 $[(CT)_{8}]$ and; Ce56fa $[(AACCG)_{5}]$.

The initial results of this inventory indicated that, for the State of Sinaloa, the genetic mangrove structure was a distance of less than 300 km. Given this, a sample of 2240 individuals was then taken to then compare amongst the main coastal aquatic systems of the State. The statistical genetic analysis showed two populations of the mangrove species *L. racemosa* and *C. erectus*: the North-Central represented by the systems between Jitzamuri-Bacorehuis and Altata-Ensenada del Pabellon, and the South represented by the systems Huizache-Caimanero and Teacapan-Agua Brava-Marismas Nacionales (see Figure 1: 1-5, 6-7, respectively). For the species *R. mangle* and *A. germinans* three populations were found: North, Central and South. The North population included systems from Jitzamuri-Bacorehuis to San Ignacio-Navachiste-Macapule (see Figure 1: 1-3). The Central population incorporated the systems of Santa Maria la Reforma and Altata-Ensenada Pabellones (see Figure 1: 4-5). The Southern population was represented by Huizache-Caimanero and Teacapan-Agua Brava-Marismas Nacionales (see Figure 1: 6-7). As a consequence of the identification of distinct populations amongst the four mangrove species distributed in Sinaloa, it was dictated by the government that the nursery-reared seedlings must be established in the influence areas of the biological populations and not permitted to be transplanted elsewhere.

Moreover, in 2007–2008 four nursery-reared seedling facilities, two in the North and two in the Central region of Sinaloa, were constructed. The mangrove plant production of these facilities is defined by the biological conditions of the mangrove species found in their local. For these green houses, mangrove plants from *R. mangle* and *A. germinans* are produced in a greater proportion than *L. racemosa* and *C. erectus* species. The reason for the difference is that *R. mangle* and *A. germinans* are the dominant species in Sinaloa and the reforestation efforts need to reflect mangrove forest structure of the natural environment.

The presence of mangrove species populations in Sinaloa provides some evidence of ecological barriers that operate at the species level. Hypothetically, the ecological barriers are represented by the partial independence of the aquatic coastal lagoons systems, but this must be tested. In addition, the North and Central systems are more physiographic limited than the South. Given this physical autonomy, which follows the dominant mangrove species in Sinaloa, it is possible that the South is more closely related to the Nayarit mangrove ecosystem. It is recommended that the genetic approach applied to the Sinaloa mangroves be expanded to other regions of Mexico. In many of these other coastal regions the mangrove restoration activities employ empirical approximation without considering the mangrove species genetic characteristics.

REFERENCES

Arenas,V., and G. de la Lanza. 1981. The effect of dried and cracked sediments on the availability of phosphorous in coastal lagoons. *Estuaries* 4 (3): 206–212.

Arriaga-Cabrera, L., E. Vázquez-Domínguez, J. González-Cano, S. Hernández, R. Jiménez-Rosenberg, E. Muñoz-López, and V. Aguilar-Sierra (coords.). 1998a. *Regiones prioritarias marinas de Mexico*. ISBN 970-9000-07-1. Comisión Nacional para el Conocimiento y Uso de la Biodiversidad. Mexico City, 198 pp.

Atlas Nacional de México. 1990. Universidad Nacional Autónoma de México. Instituto de Geografía. ISBN 968 36 1586-4. Maps: I.1.1, II.3.1, II.3.2, IV.1.1, IV.2.1, IV.3.3, IV.6.1, V.3.2 and V.4.3.

Baumert, H., and G. Radach. 1992. Hysteresis of turbulent kinetic energy in nonrotational tidal flows: A model study. *J. Geophys. Res*. 97(C3): 3669–3677.

Benitez-Pardo, D. 2004. *Creación de áreas de manglares en isletas de dragados como apoyo potencial a las pesquerías de la Bahía de Navachiste, Sinaloa. Mexico*. Informe Final. CONAPESCA, UAS, UNAM, 235 pp.

Berlanga-Robles, C.A., and A. Ruiz-Luna. 2002. Land use mapping and change detection in the coastal zone of northwest Mexico using remote sensing techniques. *Journal of Coastal Research* 18: 514–522.

Carbajal, N. 1993. *Modelling of the Circulation in the Gulf of California*. Ph.D. Dissertation, Institute of Oceanography, Hamburg University, Germany, 186 pp.

Carbajal, N., and J. O. Backhaus. 1998. Simulation of tides, residual flow and energy budget in the Gulf of California. *Oceanologica Acta* 21(3): 429–446.

Carranza-Edwards, A., M. Gutiérrez-Estrada, and R. Rodríguez-Torres. 1975. Unidades morfoterctónicas continentales de las costas mexicanas. *An. Centro Cienc. Del Mar y Limnol. Univ. Nal. Aurón. México* 2 No.1: 81–88.

Cintrón, G., Lugo, A.E., and Martínez, R., 1985. Structural and functional properties of mangrove forests. In: W.G. D'Arcy and M.D. Correa A. (eds.), *The botany and natural history of Panama.* St. Louis, MO: Missouri Botanical Garden: 53–68.

Contreras-Espinosa, F. 1993. *Ecosistemas Costeros Mexicanos*. CONABIO / Universidad Autónoma Metropolitana–Iztapalapa, Mexico City, 415 pp.

Curray, J.R., F.J. Emmel, and P.J.S. Crampton. 1969. Holocene history of a strand plain, lagoonal coast, Nayarit, Mexico. In: A. Ayala-Castañares and F.B. Phleger (eds.), *Coastal lagoons*. A Symposium (origin, dynamics and productivity). UNAM / UNESCO, Mexico City, November 28–30, 1967: 63–100.

Felix-Pico, E.F., O.E. Holguín-Quiñones, A. Hernández-Herrera, and F. Flores-Verdugo. 2006. Mangrove primary production at El Conchalito Estuary in La Paz Bay (Baja California Sur). *Ciencias Marinas* 32 (1ª): 1–11.

Flores-Verdugo, F.J., J.W. Day Jr., and R. Briseño-Dueñas. 1987. Structure, litterfall, decomposition and detritus dynamics of mangroves in a Mexican coastal lagoon with an ephemeral inlet. *Mar. Ecol. Prog. Ser*. Vol. 35: 83–90.

Flores-Verdugo, F., F. González-Farías, D.S. Zamorano, and P. Ramírez-García. 1992. *Mangrove ecosystems of the Pacific Coast of Mexico: Distribution, Structure, Litterfall and Detritus Dynamics*. In: U. Seeliger (ed.), *Coastal plant communities of Latin America. Academic Press, NY Cap.* 17: 269–287.

Flores-Verdugo, F., F. González-Farías, and U. Zaragoza-Araujo. 1993. Ecological parameters of mangroves of semi-arid regions of Mexico: Important for ecosystem management. In: H. Lieth and A. Al Masoom (eds.), *Towards the rational use of high salinity tolerant plants* 123–132.

Fuente, G., and E. Carrera. 2005. *Cambio de Uso del Suelo en la Zona Costera del Estado de Sinaloa*. Final Report to United States Forest Service (Grant No. 03-DG-11132762-157, Mexico: Ducks Unlimited de Mexico, AC, Garza García, NL).

García, E. 1973. *Modificaciones al Sistema de Clasificación Climatico de Koppen* (Adaptación a condiciones de la República Mexicana). Instituto de Geografía, UNAM, Mexico.

Inman, D.L., and C.E. Nordstrom. 1971. On the tectonics and morphologic classification of coasts. *J. Geol*. 79(1): 1–21.

Kovacs, J.M., J. Wang, and M. Blanco-Correa. 2001. Mapping mangrove disturbances using multi-date Landsat TM imagery. *Environmental Management* 27: 763–776.

Kovacs, J.M., F. Flores-Verdugo, J. Wang, and L.P. Aspden. 2004. Estimating leaf area index of a degraded mangrove forest using high spatial resolution satellite data. *Aquatic Botany* 80: 13–22.

Kovacs, J.M., J. Wang, and F. Flores-Verdugo. 2005. Mapping mangrove leaf area index at the species level using IKONOS and LAI-2000 sensors. *Estuarine Coastal and Shelf Science* 62: 377–384.

Kovacs, J.M., C. Vandenberg, and F. Flores-Verdugo. 2006. Assessing fine beam RADARSAT-1 backscatter from a white mangrove (Laguncularia racemosa (Gaertner)) canopy. *Wetlands Ecology and Management* 14: 401–408.

Kovacs, J.M., C. Vandenberg, J. Wang, and F. Flores-Verdugo. 2008a. The use of multipolarized spaceborne SAR backscatter for monitoring the health of a degraded mangrove forest. *Journal of Coastal Research* 24: 248–254.

Kovacs, J.M., C. Zhang, and F. Flores-Verdugo. 2008b. Mapping the condition of mangroves of the Mexican Pacific using C-band ENVISAT ASAR and Landsat optical data. *Ciencias Marinas* 34: 407–418.

Kovacs, J.M., J.M.L. King, F. Flores de Santiago, and F. Flores-Verdugo. 2009. Evaluating the condition of a mangrove forest of the Mexican Pacific based on an estimated leaf area index mapping approach. *Environmental Monitoring and Assessment* 157: 137–149.

Lankford, R.R. 1977. Coastal lagoons of Mexico. Their origen and classification. In: M. Wiley (ed.), Estuarine Processes. Vol 2: *Circulation, sediments and transfer of material in the estuary* 182–215.

Monroy-Torres, M. 2005. *Distribución de tres especies de manglar en relación al hidroperiodo y salinidad intersticial en el estero de Urías, Mazatlán, Sinaloa*. Tesis de Licenciatura. Facultad de Ciencias, Universidad Nacional Autónoma de México, 83 pp.

Nettel, A., F. Rafii, and R.S. Dodd, 2005. Characterization of microsatellites markers for the mangrove tree *Avicennia germinans* L. (Avicenniaceae). *Molecular Ecology Notes* 5: 103–105.

Nettel, A., R.S. Dodd, J.A.Cid-Becerra, and J. de la Rosa-Velez. 2007. Development of microsatellite markers for the white mangrove (*Laguncularia racemosa* C.F. Gaertn., Combretaceae). *Conservation Genetics* 7: 6–7.

Nettel, A., R.S. Dodd, J.A. Cid-Becerra, and J. de la Rosa-Velez. 2008. Ten new microsatellite markers for the buttonwood mangrove (*Conocarpus erectus* L., Combretaceae). *Molecular Ecology Resources* 8: 851–853.

Ortiz-Pérez, and Espinosa-Rodríguez. 1990. *Geomorphological classification of the coast of Mexico.* Geomorphology 2. Atlas Nacional de México. Instituto de Geografía, UNAM. ISBN 968 36 1586-4. Vol 2: IV.3.4.

Pearce D.W., and K.R. Turner. 1990. *Economics of natural resources and the environment*. John Hopkins University Press, 320 pp.

Rosero-Galindo, C., E. Gaitán-Solís, H. Cárdenas-Henao, J. Tohme, and N. Toro-Perea, 2002. Polymorphic microsatellites in a mangrove species, *Rhizophora mangle* L. (Rhizophoraceae). *Molecular Ecology Notes* 2: 281–283.

Schwiderski, E.W. 1980. Ocean Tides, Part I: Global Ocean Tidal Equation. *Marine Geodesy* 3: 161–217.

Serrano, D., A. Filonov, and I. Tereshchenko. 2002. Dynamic Response to Valley Breeze Circulation in Santa Maria del Oro, a Volcanic Lake in Mexico. *Geophys. Res. Lett*. 29(13): 271–274.

Strangman, A., Y. Bashan, and L. Giani. 2008. Methane in pristine and impaired mangrove soil and its possible effect on stablishment of mangrove seedling. *Biology and Fertility of soils* 44: 511–519.

Toledo, G., A. Rojas, and Y. Bashan. 2001. Monitoring of black mangrove restoration with nursery-reared seedlings on an arid coastal lagoon. *Hydrobiologia* 444: 101–109.

Twilley, R.R., and J.W. Day. 1999. The productivity and nutrient cycling of mangrove ecosystem. In: A. Yánez-Arancibia and A.L. Lara-Domínguez (eds.), *En el ecosistema del manglar en América Latina y cuenca del Caribe: su manejo y conservación*. Instituto de Ecología, AC, Xalapa, Mexico / UICN/ORMA Costa Rica / NOAA/NMFS Silver Spring MO USA, 380 pp.

UNAM. 1994. Tabla de predicción de mareas. Puertos del Pacífico. Instituto de Geofísica, Mexico.

Walters, B.B., P. Ronnback, J.M. Kovacs, B. Crona, A. Hussain, R. Badola, J. Primavera, E. Barbier, and F. Dahdouh-Guebas. 2008. Ethnobiology, socio-economics and management of mangroves: A review. *Aquatic Botany* 89: 220–236.

[1] Unidad Académica Mazatlán, Instituto de Ciencias del Mar y Limnología, Universidad Nacional Autónoma de México, Mazatlán, Sinaloa, México, ffverdugo@gmail.com

[2] Department of Geography, Nipissing University, North Bay, ON, Canada, johnmk@nipissingu.ca

[3] Facultad de Ciencias del Mar, Universidad Autónoma de Sinaloa, Mazatlán, Sinaloa, México, davidse65@yahoo.com

[4] Departamento de Ciencias Biológicas, Universidad de Occidente, Unidad Los Mochis, Los Mochis, Sinaloa, México, jcid@mochis.udo.mx

Exploring Mexico's northwest, the Baja California Peninsula, its surrounding oceans, its islands, its rugged mountains, and rich seamounds, one feels diminished by the vastness and the greatness of the landscape while consumed by a sense of curiosity and awe. In a great natural paradox, we see the region's harsh arid nature molded by water through deep time, and we feel that its unique lifeforms have been linked to this desert and sea for thousands of years, as they are now.

These landscapes of fantasy and adventure, this territory of surprising, often bizarre growth-forms and of immense natural beauty, has inspired a wide array of research for over two centuries and continues to inspire the search for a deeper knowledge on the functioning, trends, and conservation status of these ecosystems in both land and ocean.

This book offers a compilation of research efforts aimed at understanding this extraordinary region and preserving its complex richness. It is a synthesis of work done by some exceptional researchers, mostly from Mexico, who indefatigably explore, record, and analyze these deserts and these seas to understand their ecological processes and the role of humans in their ever-changing dynamics.

Elisabet V. Wehncke

UC MEXUS
The University of California Institute for Mexico and the United States

SEMARNAT
SECRETARÍA DE MEDIO AMBIENTE Y RECURSOS NATURALES

ESTADOS UNIDOS MEXICANOS

INECC
INSTITUTO NACIONAL DE ECOLOGÍA Y CAMBIO CLIMÁTICO

ISBN 978-1-4951-2222-4
90000
9 781495 122224